that a much lower value could be computed. Therefore, both OH rupture and 1,2-H_2 elimination could be competitive events from the n,3s singlet state of methanol. However, the electronically adiabatic CH rupture and 1,1-H_2 elimination should occur only at much higher than UV threshold excitations. The relationship between the theoretical observations and the already discussed confused state of the experimental work[4] cannot be fully established. We find that the repulsive natures of the OH surfaces in both the n,3s singlet and triplet states eliminate these states as being metastable in character. The IR multiphoton photochemistry of methanol[31] shows either CO rupture or H_2 elimination, whereas the UV photochemistry shows mainly OH rupture. Therefore, vibrationally hot ground state methanol cannot fully serve as a possible intermediate in the UV photochemistry except as generated by CH_3O + H recombination. Therefore, a reinvestigation of the experimental UV photochemistry of methanol is necessary to better establish if in fact a metastable species exists.

C. Final Comments. We only discussed the possibility of CN and NH bond ruptures in the case of methylamine photochemistry. By analogy with the above calculations on methanol and ammonia[40a] one anticipates several other processes.[4] As in the case of methanol, we anticipate adiabatic CH rupture to be endoergic from the n,3s state, giving a Rydberg excited radical fragment, CH_2NH_2*. Likewise, we anticipate H_2[4,40a] eliminations to give CH_3N, $CHNH_2$, CH_2=NH to be high barrier transformations from the n,3s singlet or triplet states, which are lower in energy than in methanol with regard to product states. These processes will adiabatically occur at higher excitation energies. The fact that methylamine photochemistry only displays NH rupture in the UV absorption threshold region is, therefore, easily rationalized as a process occurring directly from the electronically excited state. Likewise, the threshold stability of excited trialkylamines is easily rationalized on the basis of our computations. However, the recently observed lack of kinetic energy in the fragments obtained in the photochemistry of trimethylamine[22] at much higher than threshold excitations indicates that the reacting species is the vibrationally hot ground state. Therefore, whereas we anticipate a direct, high barrier, excited state CN bond rupture in trialkylamines, other nonradiative processes may be intervening to take the system to the vibrationally excited ground state before the CN exit channel is achieved. These observations lead us to caution the reader to use the theoretical analysis presented here in the following manner. In the case of NH or OH bond ruptures in n,3s excited amines and alcohols, the barriers are low or do not exist. In this case the excited state reactions should be either direct or predissociative. The CO excited state ruptures in alkyl and alicyclic ethers may be similar. But for those other processes which have high barriers, the calculations should only be taken as indications that difficulties are encountered along these pathways and that other nonradiative processes could occur which could lead the system in the same direction.

Registry No. Methanol, 67-56-1; methylamine, 74-89-5; ammonia, 7664-41-7.

A Theoretical Study on the Photochemical Transposition Reaction of Oxazole

Hidetsugu Tanaka, Toshio Matsushita, and Kichisuke Nishimoto*

Contribution from the Department of Chemistry, Faculty of Science, Osaka City University, Sumiyoshi-ku, Osaka 558, Japan. *Received July 19, 1982*

Abstract: The photochemical transposition reaction of oxazole (interchange of positions 2 and 3, 4 and 5, 2 and 4, or 3 and 5) is investigated by ab initio MO-CI calculation. The present calculation shows that a 1-azirine intermediate in the S_1 state is formed from the lowest $^1(n \rightarrow \pi^*)$ state of oxazole with the out-of-plane distortion. Then, the intersystem crossing (ISC) to the T_1 state gives rise to the interchange of positions 2 and 3 to yield isoxazole. On the other hand, the lowest $^1(\pi \rightarrow \pi^*)$ state of oxazole brings about two types of transpositions, i.e., the 4,5 transposition and the 2,4 and 3,5 transpositions. Positions 4 and 5 are interchanged via a 2-azirine intermediate when the out-of-plane distortion at this state and the internal conversion to the S_1 state occur. On the other hand, the 2,4 or 3,5 transposition is caused by the sigmatropic shift of an oxygen atom when a bicyclic intermediate is formed with the disrotatory ring closure and subsequent ISC to the T_1 state.

Considerable attention has been focused in recent years on the photochemistry of five-membered heterocyclic ring systems.[1] Most of them have been related to the isomerization reactions that result in an interchange of ring atoms.[2] For instance, it is well-known that irradiation of furans[3] or isoxazoles[4,5] causes the interchange of positions of adjacent ring atoms. These photoisomerizations can be interpreted by the reaction course via the three-membered-ring intermediate formation (ring contraction–ring expansion mechanism).[2]

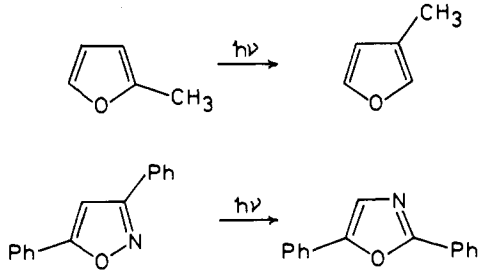

In a previous paper, we succeeded in elucidating the reaction mechanism of photochemical rearrangement of isoxazoles to oxazoles and explained the wavelength-dependent photochemistry of the 1-azirine intermediates by ab initio MO-CI calculation.[5]

Oxazoles, being the products in photochemical rearrangement of isoxazoles, also undergo the molecular reorganization under the influence of UV–visible light. For example, irradiation of 2,5-diphenyloxazole (**1b**) in ethanol gave 4,5-diphenyloxazole (**9b**, transposition of atoms 2 and 4) and 3,5-diphenylisoxazole (**3b**, transposition of atoms 2 and 3). When **1b** was irradiated in

(1) Lablache-Combier, A. "Photochemistry of Heterocyclic Compounds"; Bachardt, O., Ed.; Wiley: New York, 1976: p 123.
(2) Padwa, A. "Rearrangements in Ground and Excited States"; de Mayo, P., Ed.; Academic Press: New York, 1980; Vol. 3, p 501.
(3) Hiraoka, H.; Srinivasan, R. *J. Am. Chem. Soc.* **1968**, *90*, 2720. Hiraoka, H. *J. Phys. Chem.* **1970**, *74*, 574.
(4) Singh, B.; Zweig, A.; Gallivan, J. B. *J. Am. Chem. Soc.* **1972**, *94*, 1199 and references cited therein.
(5) Tanaka, H.; Osamura, Y.; Matsushita, T.; Nishimoto, K. *Bull. Chem. Soc. Jpn.* **1981**, *54*, 1293.

0002-7863/83/1505-1753$01.50/0

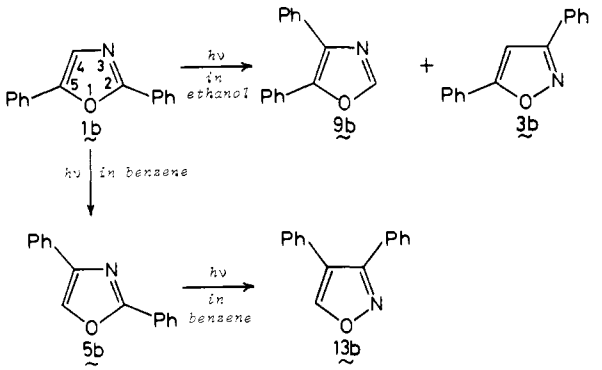

benzene, 2,4-diphenyloxazole (**5b**, transposition of atoms 4 and 5) was obtained. Further irradiation of **5b** in benzene produced 3,4-diphenylisoxazole (**13b**) in good yield.[6] (In the case of 2-methyl-5-phenyloxazole, the transposition of atoms 3 and 5 was also observed.)

This light-induced reaction is more complex than that of isoxazoles and cannot be explained with the ring contraction–ring expansion mechanism. The phototranspositions of oxazoles can be divided into two types. One of them involves the interchange of two adjacent atoms (type A). The other one (type B) consists of rearrangements involving the exchange of positions 2 and 4 and of positions 3 and 5. The substituents of the oxazole ring seem also to play an important role in controlling the course of rearrangement. In addition, the photobehavior of the system might be affected by the nature of the solvent employed.

In the present study, the reaction mechanisms of 2,3-, 4,5-, 2,4-, and 3,5-transposition reactions of oxazoles are investigated by ab initio MO-CI calculations in which oxazole (**1a**) is used as a model system. In this work, the following reaction intermediates (or transient species) are assumed:

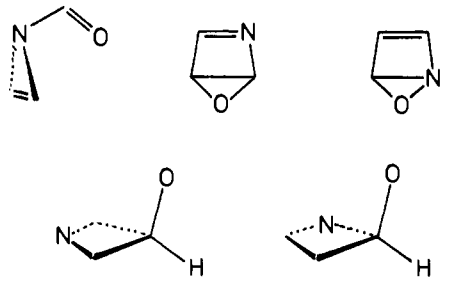

It has been suggested that azirines are involved in the photochemical rearrangements of oxazoles, which proceed with the interchange of adjacent ring atoms.[2] 1-Azirines were isolated as the products from the crude reaction mixture.[6] On the other hand, 2-azirines have not yet been isolated or detected because of their intrinsic instability that arises from their antiaromatic character.[7] Dewar oxazoles and Dewar isoxazoles, which are the same types of interemediates as in the photoisomerization of thiophenes, might be important reaction intermediates.[8,9] Four-membered-ring species are supposed to be the transition-state species of a [1,3]-sigmatropic shift of an oxygen atom. Therefore, it is of interest to calculate the geometries and the electronic structures of these species.

We assumed the following four reaction paths of the transpositions of oxazoles:

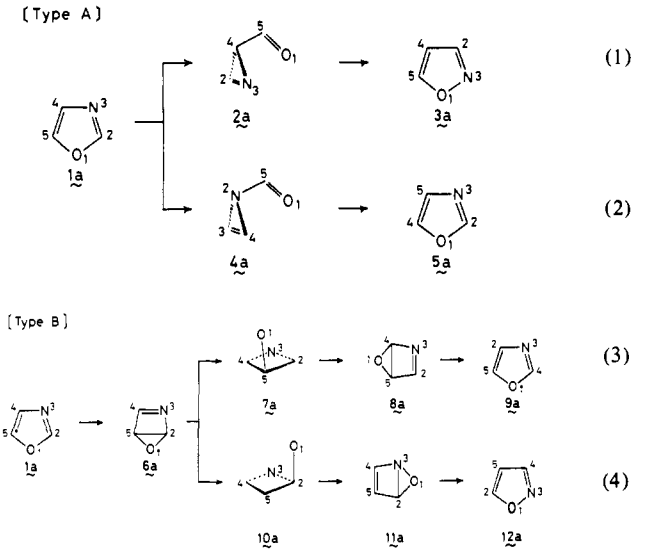

We then calculated the potential curves for these paths and will discuss what types of intermediates (or transients) are involved in these photoreactions and whether two types of products (type A and type B) can arise from the same excited state.

Calculations

The ground-state geometries are calculated with the STO-3G minimal basis set.[10] The excited-state geometries are calculated within the singly excited configuration interaction (SECI) procedure in which all the singly excited configurations except the inner-shell excitations are included (the singly valence excited configurations).

We cannot describe sufficiently the bond breaking or making only in terms of single configuration. Thus, the ground-state potential curves are calculated with a CI method including all the singly valence excited configurations and doubly excited configurations from five highest occupied (HO) MO's and five lowest unoccupied (LU) MO's (SDCI). The excited-state potential curves are calculated with a CI method including SDCI plus triply excited configurations from four HOMO's and three LUMO's (SDTCI).

The configuration selection may sometimes cause the correlation effect to be unbalanced at each point of potential curves. But the present CI calculation takes the possible configurations related to the bond breaking or making into consideration and, therefore, could describe the important features of the reactions.

Results and Discussion

A. Electronic Structures of the Reactant, Products, and Hypothetical Intermediates. The optimized ground-state geometries of the reactant, products, and hypothetical intermediates and the excited-state geometries of some species are shown in Figure 1. The energy levels of the ground (S_0) and some low-lying excited states calculated by SECI method are shown in Figure 2.

1a and 3a. The T_1, T_2, T_4, and S_2 states of **1a** and **3a** are $\pi \rightarrow \pi^*$ states (A′), and their T_3 and S_1 states are $n \rightarrow \pi^*$ states (A″).

Figures 1b and 1c show the optimized geometries of two lowest excited singlet states of **1a**, $^1A''$ and $^1A'$ states. For comparison, that of the ground state is also shown in Figure 1a. These figures show the geometrical changes of **1a** due to the excitation. Considerable changes in the C_2–N_3 bond length and the C_2–N_3–C_4 and the O_1–C_2–N_3 bond angles in the $^1A''$ state (see Figure 1b) may suggest that this excitation is almost localized at the C_2–N_3 bond. On the other hand, in the $^1A'$ state one can see the enlargements of the C_2–N_3 and C_4–C_5 bonds and the shortening of the N_3–C_4 bond. These features may be responsible for yielding two types of products. Characteristics and geometries of the excited states of **3a** are similar to those of **1a**.[5]

(6) Kojima, M.; Maeda, M. *Trahedron Lett.* **1969**, 2379; *J. Chem. Soc., Chem. Commun.* **1973**, 539. Maeda, M.; Kojima. M. *J. Chem. Soc., Perkin Trans. 1* **1977**, 239.
(7) Torres, M.; Lown, E. M.; Gunning, H. E.; Strausz, O. P. *Pure Appl. Chem.* **1980**, *52*, 1623.
(8) Wynberg, H.; Kellogg, R. M.; Van Driel, H.; Beekhuis, G. E. *J. Am. Chem. Soc.* **1967**, *89*, 3501 and references cited therein.
(9) Matsushita, T.; Osamura, Y.; Tanaka, H.; Nishimoto, K., to be published.
(10) IMS library program IMSPAC is used.

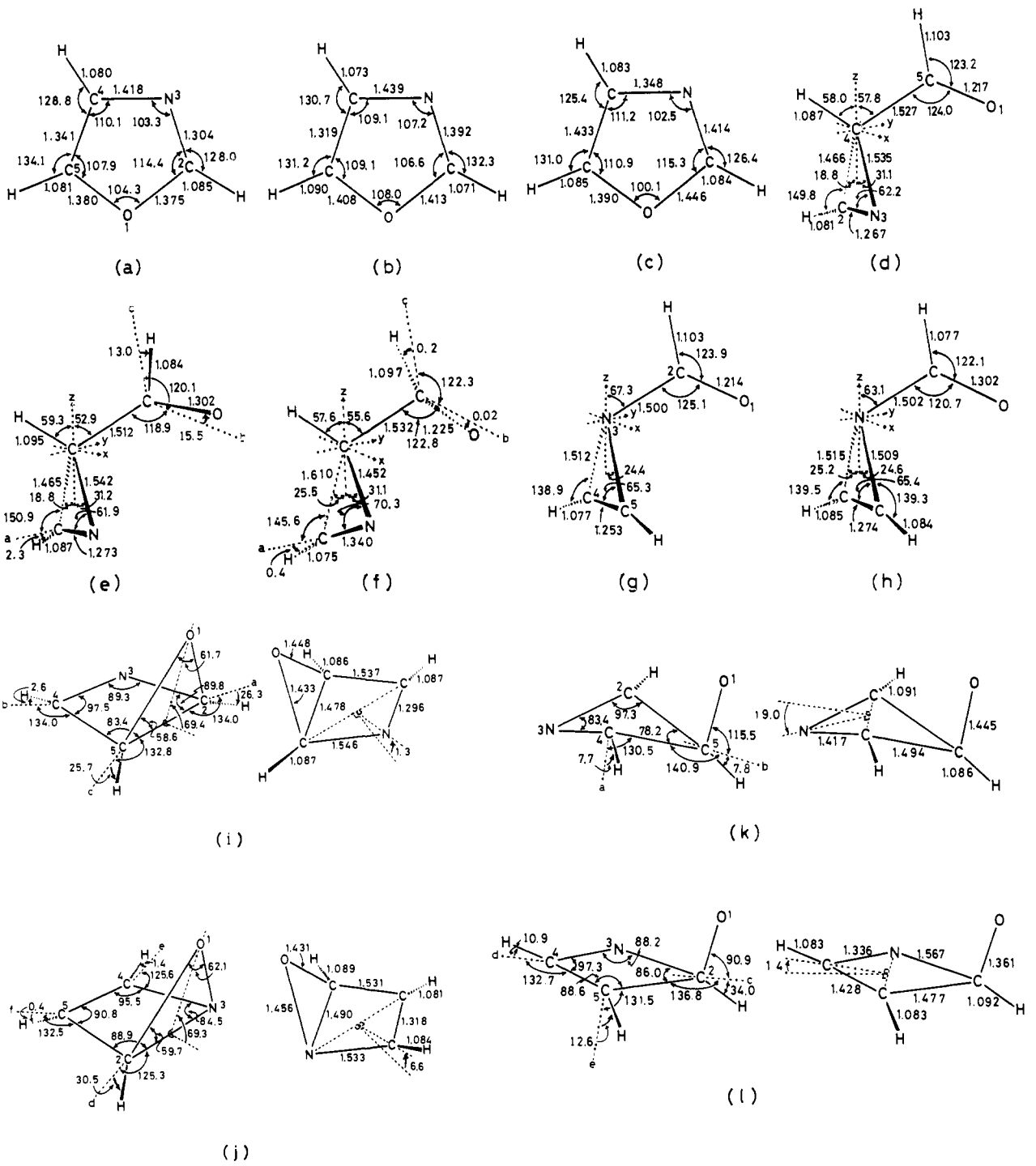

Figure 1. Optimized ground-state geometries of all species and excited-state geometries of some species calculated with the SCF and SECI method. Units are in angstroms and degrees.

2a and 4a. The optimized ground-state geometry of **4a** is shown in Figure 1g. Upon optimization, **4a** is assumed to have a C_s symmetry. For comparison, the geometry of **2a** is given in Figure 1d.[5]

The S_1 state of **2a** is assigned to be an $n \rightarrow \pi^*$ state of the C=O chromophore and the S_2 state to an $n \rightarrow \pi^*$ state of the C=N chromophore. Thus, these states are almost localized at each chromophore (see Figure 1, e and f, which are structures optimized with the SECI method). This is one of the reasons that **2a** has a wavelength-dependent photochemistry.[5]

2-Azirine (a parent molecule of **4a**) together with oxirene and thiirene is known to be a $4n$ π-electron antiaromatic heterocyclic analogue of cyclobutadiene and, therefore, inherently unstable. These species have been of interest both experimentally and theoretically.[7]

As Figure 1g shows, the C–N bond distance of **4a** is much longer than the standard value (1.40 Å), which is same as that in 2-azirine, oxirene, or thiirene.[11-13] This probably reflects the tendency to reduce destabilizing conjugation. In addition, the distortion at the N atom from the planarity also reduces the antiaromatic interaction. 2-Azirine has not been detected or isolated yet, since it undergoes facile 1,2-hydrogen shift to form 1-azirine.[14] In the case of **4a**, however, the C–N bond scission

(11) Hopkinson, A. C.; Lien, M. H.; Yates, K.; Csizmadia, I. G. *Int. J. Quantum Chem.* **1977**, *12*, 355.
(12) Strausz, O. P.; Gosavi, R. K.; Gunning, H. E. *Chem. Phys. Lett.* **1978**, *54*, 510.
(13) Strausz, O. P.; Gosavi, R. K.; Bernardi, F.; Mezey, P. G.; Goddard, J. D.; Csizmadia, I. G. *Chem. Phys. Lett.* **1978**, *53*, 211.
(14) Clark, D. T. *Theor. Chim. Acta* **1969**, *15*, 225.

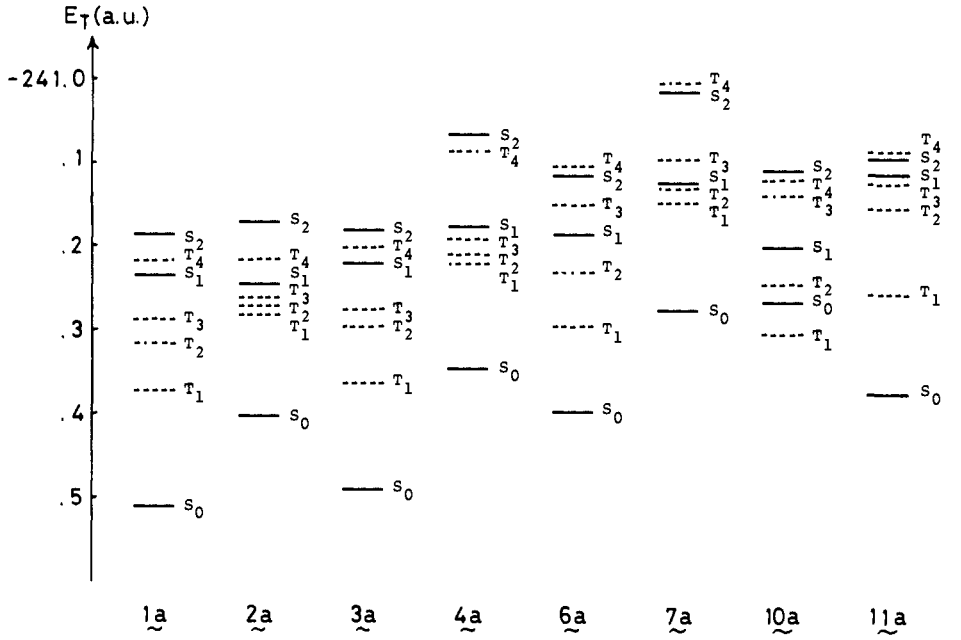

Figure 2. State energies of the ground (S_0) and some low-lying excited states calculated by the SECI method.

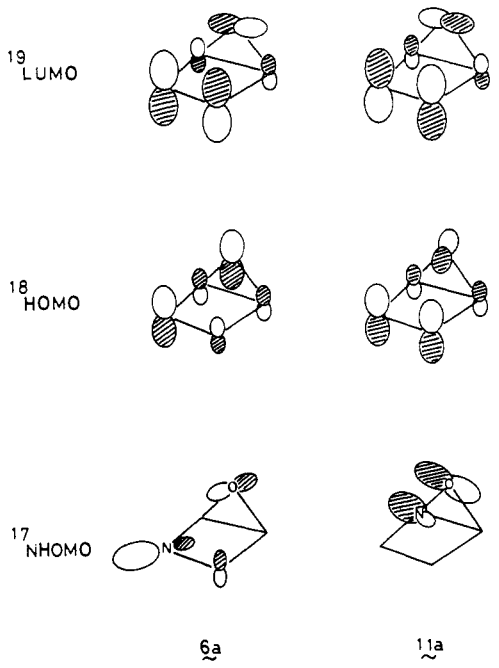

Figure 3. Schematic descriptions of some active MO's of **6a** and **11a**.

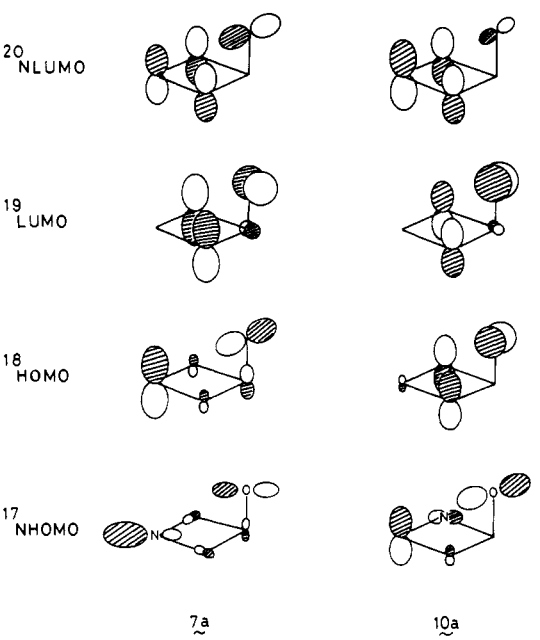

Figure 4. Schematic descriptions of some active MO's of **7a** and **10a**.

of the azirine ring occurs easily to give oxazole, which will be discussed later. **4a** is computed to be less stable than **2a** by ca. 36 kcal mol^{-1}, which is almost same as the energy difference between 2-azirine and 1-azirine.[11]

The T_1 and S_2 states of **4a** are $\pi \rightarrow \pi^*$ states of the C=C chromophore, while the T_2 and S_1 states are $n \rightarrow \pi^*$ states of the C=O chromophore. Figure 1h shows the optimized structure of **4a** at the S_1 state. One can see that this excitation is almost localized at the C=O chromophore and the C_s symmetry is broken slightly. This suggests that **4a** in the S_1 state easily collapses to give **5a** or **1a**.

6a and 11a. Figure 1, i and j, shows the optimized ground-state structures of **6a** and **11a**, respectively. The structure of the epoxide part of **6a** is similar to that of oxirane,[15] whereas that of the oxaziridine part of **11a** is appreciably different from that of oxaziridine derivatives.[16] Thus, the O_1–N_3 bond of **11a** is shorter than that of oxaziridine derivatives, while the C_2–N_3 bond is longer. This implies that the C–N bond in **11a** is weaker and easier to break than the O–N bond, which is contrary to oxaziridine derivatives.

The weights of predominant configurations in the T_1 and S_1 states of **6a** and **11a** are T_1 (**6a**) $\simeq$ 0.80 (18 $\rightarrow$ 19) + 0.33 (17 $\rightarrow$ 19) − 0.33 (15 $\rightarrow$ 19), S_1 (**6a**) $\simeq$ 0.73 (17 $\rightarrow$ 19) − 0.57 (18 $\rightarrow$ 19), T_1 (**11a**) $\simeq$ 0.90 (18 $\rightarrow$ 19) + 0.23 (16 $\rightarrow$ 19), and S_1 (**11a**) $\simeq$ 0.76 (17 $\rightarrow$ 19) − 0.31 (17 $\rightarrow$ 20) − 0.29 (18 $\rightarrow$ 19) − 0.29 (16 $\rightarrow$ 19), where (18 $\rightarrow$ 19) means the singly excited configuration from the 18th MO to the 19th MO, and so on. The

(15) Cunningham, G. L., Jr.; Boyd, A. W.; Myers, R. J.; Gwinn, W. D.; Le Van, W. I. *J. Chem. Phys.* **1951**, *19*, 676. Lord, R. C.; Nolin, B. *Ibid.* **1956**, *24*, 656.

(16) Jerslev, B. *Acta Crystallogr.* **1967**, *23*, 645. Cannon, J. F.; Daly, J.; Silverton, J. V.; Boyed, D. R.; Jerina, D. N. *J. Chem. Soc., Perkin Trans. 2* **1972**, 1137. Oliveros, E.; Riviere, M.; Malrieu, J. P.; Teichteil, Ch. *J. Am. Chem. Soc.* **1979**, *101*, 318. Bigot, B.; Roux, D.; Sevin, A.; Devaquet, A. *Ibid.* **1979**, *101*, 2560.

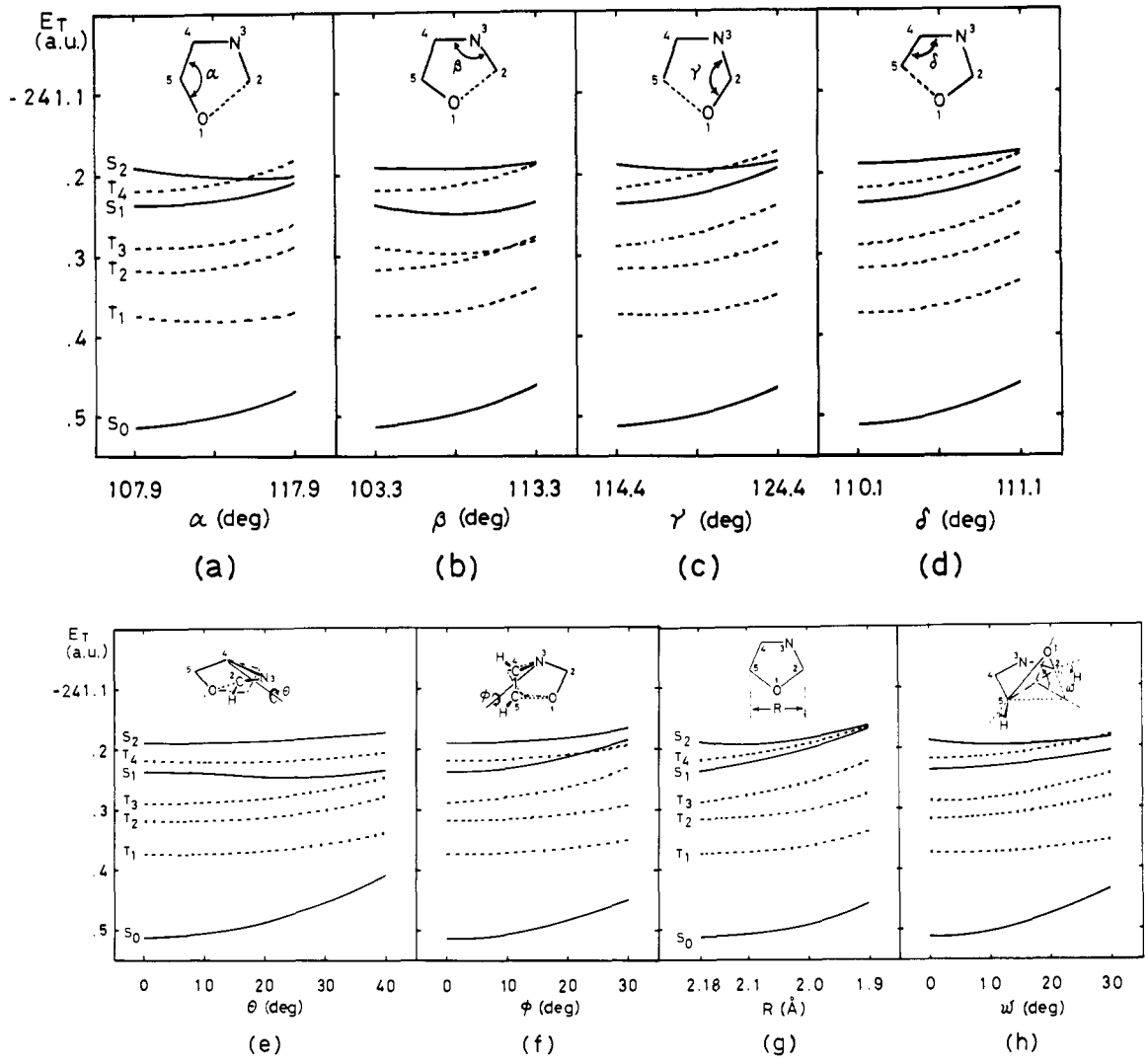

Figure 5. State energy variations of **1a** by the deformations responsible for intiating the reaction (see text).

shapes of some active MO's (17 to 19) of **6a** and **11a** are shown in Figure 3. From this figure, it is expected that the structures of **6a** in the T_1 and S_1 states are similar to those of the ground state except the enlargement of the C_2–C_5 and N_3–C_4 bond lengths. On the other hand, the C_2–N_3 bond of **11a** is much longer in the T_1 or S_1 state. In fact, the computed results show that **11a** in the S_1 state is not stable, which causes ring opening to give isoxazole.

7a and 10a. The optimized ground-state geometries of **7a** and **10a** are shown in Figure 1, k and l. Upon optimization, some restrictions are imposed on the structures of **7a** and **10a**. C_s symmetry is assumed for **7a**. On the other hand, the C_2–N_3–C_5 and O_1–C_2–H planes are assumed to be perpendicular to each other for **10a**. When these restrictions are removed, **7a** or **10a** leads to the bicyclic intermediate **6a**, **8a**, or **11a** upon optimization. This suggests that **7a** and **10a** are the transition states of oxygen atom migration reactions **6a** → **8a** or **6a** → **11a** at the SCF level.

The electron assignments of **7a** and **10a** in the ground states are as follows:

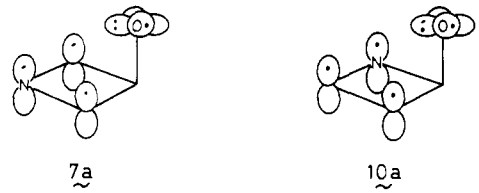

7a ~ 10a ~

Therefore, one can see from these structures that the O_1–C_4 (C_2) bond formation (**7a** → **8a** (**6a**)) and the O_1–N_3 (C_5) bond formation (**10a** → **11a** (**6a**)) occur easily at the ground state.

The weights of the predominant configurations in the T_1 and S_1 states of **7a** and **10a** are T_1 (**7a**) ≃ 0.94 (18 → 19) + 0.22 (17 → 19), S_1 (**7a**) ≃ 0.95 (18 → 19) + 0.23 (17 → 19), T_1 (**10a**) ≃ 0.96 (18 → 19) − 0.12 (16 → 19), and S_1 (**10a**) ≃ 0.90 (17 → 19) + 0.34 (15 → 19). The shapes of some active MO's (17 to 20) of **7a** and **10a** are shown in Figure 4. This figure suggests at the SCF and SECI levels that **7a** or **10a** is hard to form the O_1–C_4 (C_2) or O_1–N_3 (C_5) bond at the T_1 or S_1 state.

B. Preliminary Consideration for the Reaction Coordinate of Each Path. In order to infer the reaction coordinate of each path, we examined the relation between the geometric deformations and the state energy variations in the low-lying states of **1a**. Several geometric parameters responsible for each reaction path are varied independently from the ground-state equlibrium geometry. The results are shown in Figure 5.

Increase of the C_2–N_3–C_4 bond angle (β) stabilizes the S_1 state (Figure 5b) and of the C_4–C_5–O_1 (α) or the O_1–C_2–N_3 bond angle (γ) stabilizes the S_2 state (Figure 5, a and c). The stabilization in the S_1 or S_2 state can be interpreted by Walsh's rule.[17] Thus, the distoriton of the C_4–N_3–C_2 part with the out-of-plane motion (θ) that varies the hybridization of the C_4 atom (sp^2 → sp^3) stabilizes the S_1 state (Figure 5e), while that of the N_3–C_4–C_5 part (ϕ) varying the hybridization of the N_3 atom (sp^2 → sp^3) does not stabilize any states (Figure 5f). This result suggests that path 1 proceeds in the S_1 state with the geometric deformation

(17) Walsh, A. D. *J. Chem. Soc.* **1953**, 2260.

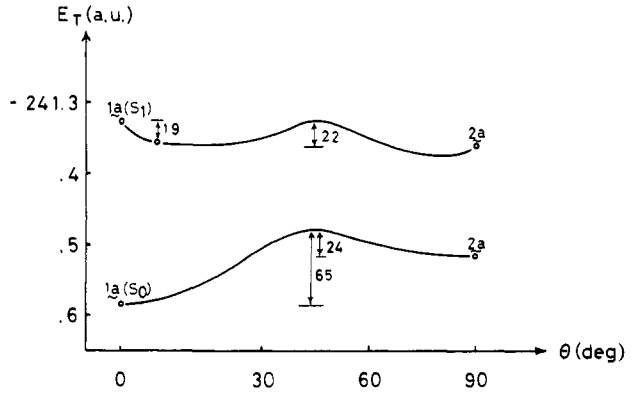

Figure 6. Energy profile of minimum energy path along θ for path 1 (**1a** → **2a**). The height of energy barriers are in kcal mol^{-1}.

θ, while path 2 does so in the S_2 state with γ and subsequently with ϕ.

Decrease of the C_2–C_5 distance (R) or the disrotatory deformation of the HC_5–O_1–C_2H part (ω) stabilizes the S_2 state (Figure 5, g and h), which can be explained from the shapes of the singly occupied (SO) MO's. One may expect that paths 3 and 4 are initiated in S_2 state with the decrease of R and the deformation of ω to yield the bicyclic intermediate **6a**.

C. Minimum-Energy Path of Each Reaction Path. In order to obtain the minimum-energy path of each path, we optimized the geometries at the ground and excited states along the reaction coordinate infered from the results of the previous section with the SDCI and SDTCI calculations. Upon optimization, the C–H bond distances and the bond angles or dihedral angles related to the hydrogen atoms are fixed in so far as the hybridization of the carbon atom is unchanged in the course of the reaction.

Path 1. Figure 6 shows the potential curves along the geometric parameter θ (**1a** → **2a**). The values in this figure are the height of the barrier in kcal mol^{-1}. The second circle of the S_1 curve corresponds to the optimized structure of **1a** at the S_1 state (see Figure 1b).

The height of the energy barrier at the S_1 state is calculated to be 22 kcal mol^{-1}. This value is too large compared with the value estimated by Turro.[18] But this barrier may be lowered by the inclusion of the environment effect or the substituent effect. We can expect that the conjugation between a σ radical and an aromatic substituent lowers the energy barrier when an aromatic substituent is on the C_2 atom and is twisted by $\pi/2$ from the oxazole plane. In fact, experiments show that 2-phenyloxazole gives rise to a 2,3 transposition, whereas 4-phenyloxazole or 5-phenyloxazole does not.[6]

Once the system goes over the barrier, **2a** in the S_1 state is easily formed, as seen from Figure 6. **2a** in the S_1 state goes to the T_1 state by the intersystem crossing (ISC) and gives the product **3a**. When the deactivation from the S_1 to the ground states occurs, **2a** is also obtained as a product, which was discussed in our previous paper.[5]

Turning to the ground-state reaction, the energy barrier of **1a** → **2a** is calculated to be 65 kcal mol^{-1}, whereas that of **2a** → **1a** is 24 kcal mol^{-1}. This result implies that the reaction **1a** → **2a** does not occur thermally and the reverse reaction **2a** → **1a** can occur in these severe experimental condition.[6]

Path 2. Figure 7 displays the potential energy profile along the geometric parameter ϕ (**1a** → **4a** → **5a**). The second circles in the S_1 and S_2 curves correspond to the optimized structures at these states (ϕ = 0.0°).

The out-of-plane distortion ϕ gives rise to mixing between the S_1 and S_2 states and, at $\phi \simeq 20°$, the characters of these states are interchanged with each other. One may expect that the internal conversion (IC) from the S_2 to the S_1 states occurs at this region. Once the IC occurs, the S_1 potential curve is connected

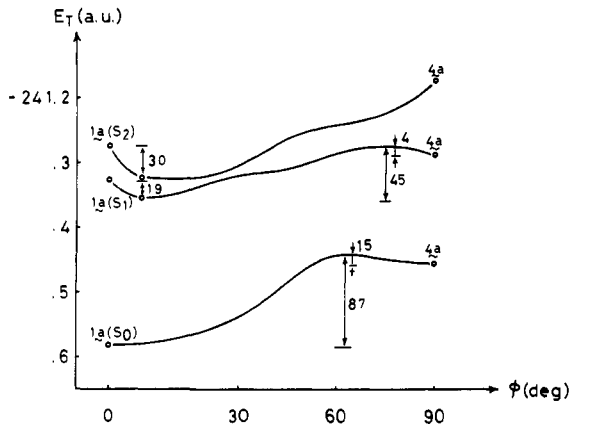

Figure 7. Energy profile of minimum energy path along ϕ for path 2 (**1a** → **4a** → **5a**).

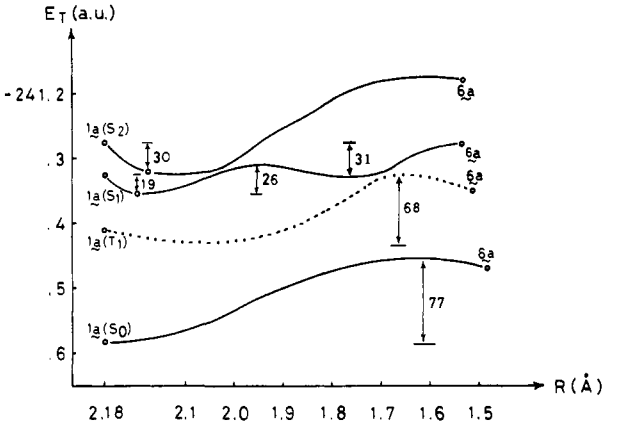

Figure 8. Energy profile of minimum energy path along R for the first step of paths 3 and 4 (**1a** → **6a**).

to **4a** in the S_1 state with the calculated activation energy of 24 kcal mol^{-1}. When an aromatic substituent is on the C_5 atom, the conjugation between σ radical and an aromatic substituent might lower this energy barrier and make the 4,5 transposition easy to proceed.

Since the S_1 state of **4a** is an n → π^* state of the C=O chromophore, the electron populated on the C_2 atom can delocalize into the σ-type LUMO of azirine ring. In addition to the strain and the antiaromaticity of azirine ring, this type of orbital interaction could promote N–C bond scission. The calculated results indicate that **4a** in the S_1 state proceeds to form the C–O bond with concerted manner and gives **5a** or **1a** without any intermediacy such as iminocarbene.

Thermal reaction of **1a** → **4a** is calculated to require an activation energy of 87 kcal mol^{-1}, while the reverse reaction (**4a** → **5a** (**1a**)) takes 15 kcal mol^{-1}. The small value for the latter is due to ring strain and the antiaromaticity of 2-azirine and indicates that **4a** in the ground state is converted to **5a** or **1a** easily, even if the deactivation from the S_1 to the ground states occurs.

Paths 3 and 4. Each reaction path consists of three steps. The first step is a ring closure of **1a** to give a bicyclic intermediate (**1a** → **6a**), the second is a sigmatropic shift of oxygen atom (**6a** → **7a** → **8a** and **6a** → **10a** → **11a**), and the third is the ring opening of **8a** or **11a** (**8a** → **9a** and **11a** → **12a**).

As discussed in the previous section, the shapes of SOMO's at the S_2 state suggest that the disrotatory ring closure of **1a** causes the formation of a bicyclic intermediate. Figure 8 displays the energy profile of the first step of paths 3 and 4, where R is the C_2–C_5 distance.

When R is decreased, the S_1 and S_2 states mix with each other. At $R \simeq 2.0$ Å, the characters of these states are interchanged (the S_1 state has $\pi \rightarrow \pi^*$ character). Thus, the IC from the S_2 to the S_1 states is expected at this region. The S_1 potential curve has a minimum at $R \simeq 1.8$ Å and is connected to the S_1 state

(18) Turro, N. J. "Modern Molecular Photochemistry"; Benjamin/Cummings: Menlo Park, CA, 1978; Chapter 8.

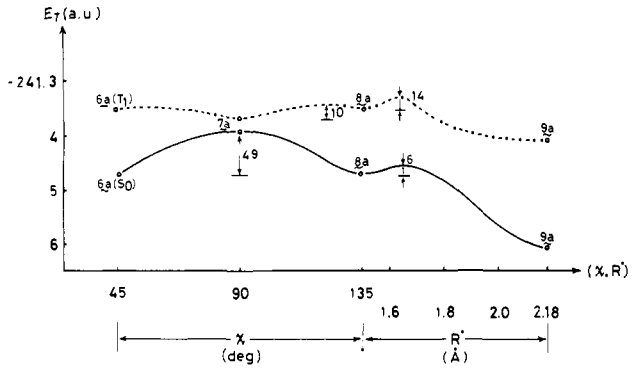

Figure 9. Energy profile of minimum energy path along χ and R' for the second and third steps of path 3 (**6a** → **7a** → **8a** → **9a**).

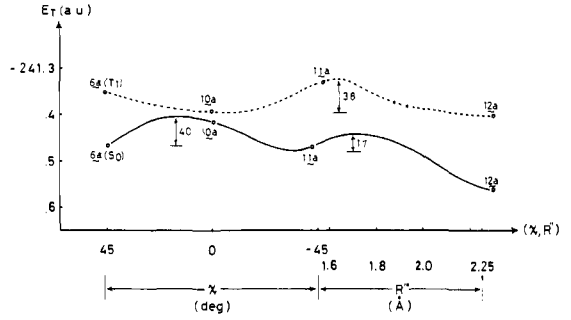

Figure 10. Energy profile of minimum energy path along χ and R'' for the second and third steps of path 4 (**6a** → **10a** → **11a** → **12a**).

of **6a** with the calculated energy barrier of 31 kcal mol^{-1}. This value seems to be large, and the reaction might not proceed via **6a** at the S_1 state.

Let us examine an alternative reaction course that does not experience a bicyclic intermediate. Se chose the O_1–C_5–a angle (ϵ) as the coordinate for the conversion to **7a** and O_1–C_2–a (η) for that to **11a** and calculated the S_1 potential curve starting at

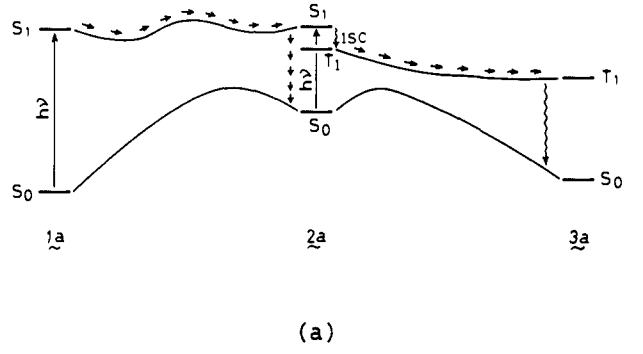

(a)

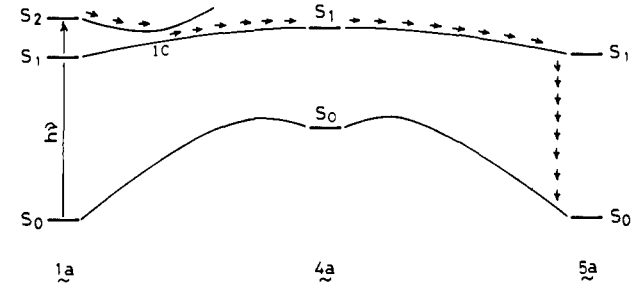

(b)

R = 1.8 Å. The results, however, do not give favorable potential curves. Therefore, we abandoned this possibility.

It is of interest to see that the S_1 and T_1 potential curves get close at $R \simeq 1.7$ Å. In addition, the S_1 and T_1 states in this region have $\pi \rightarrow \pi^*$ character. Thus, we expect that the ISC occurs and yields **6a** in the T_1 state.

As a coordinate to describe the second step of paths 3 and 4, the azimuthal angle χ is chosen (see the above figure). Figure 9 shows the energy profile for the second and third steps of path 3, where R' is the C_4–C_5 distance, which is a coordinate of the third step. As seen from this figure, **6a** in the T_1 state converts to **8a** with the calculated activation energy of 10 kcal mol^{-1} via **7a**. On the other hand, the transformation **6a** → **7a** → **8a** at the ground state is calculated to require an activation energy of 49 kcal mol^{-1}. It is of interest to see that **6a** in the ground state would be a transition state and **6a** in the T_1 state is the reaction intermediate of the sigmatropic shift of oxygen atom. Thus, we expect that the ISC from the T_1 to the ground states occurs at the region χ = 90.0° (**7a**) to give **8a**. Once **8a** is formed, the ring opening proceeds easily to yield a product, **9a**.

Energy profiles for the second and third steps of path 4 are shown in Figure 10, where R'' is the C_2–N_3 distance. This figure shows that the T_1 potential curve is descending from χ = 44.6° to 0.0° (**6** → **10a**) and ascending from χ = 0.0° to −46.7° (**10a** → **11a**). This result suggests that in the T_1 state **10a** is formed easily but **11a** is not. That is, the conversion **10a** → **11a** → **12a** is calculated to require an activation energy of 38 kcal mol^{-1}.

It is expected that the ISC from the T_1 to the ground states occurs at the region χ = 0.0°. Once the ISC occurs, the conversion to a product, **12a**, proceeds easily since the system has enough

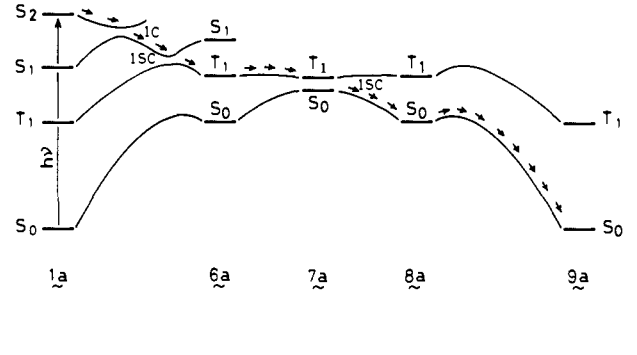

(c)

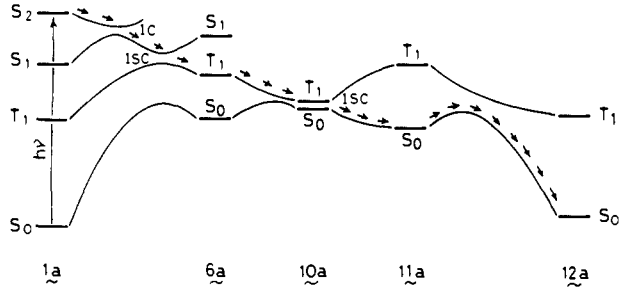

(d)

Figure 11. Schematic descriptions of possible reaction mechanisms for (a) path 1, (b) path 2, (c) path 3, and (d) path 4 infered from the present calculations.

energy to go over the barrier of ring opening (17 kcal mol^{-1}). It is noteworthy to see that in the ground state **10a** is not a transition state in the conversion **6a** → **11a**. This is a result obtained by including singly and doubly excited configurations.

Let us discuss the influence of the substituent upon the reaction courses of paths 3 and 4. When an aromatic substituent is on the C_2 or C_5 atom, the amplitudes of p_π AO's of LUMO on these atoms increase. Therefore, the bicyclic intermediate formation is favorable in the $\pi \rightarrow \pi^*$ state of 2-aryloxazole (**1c**) or 5-aryloxazole (**1d**). In addition, the stabilization due to the conjugation effect with a substituent might play an important role in the determination of the reaction course. **7c** (or **10d**) is conjugated between an aromatic substituent and the C_2–N_3–C_4 (or N_3–C_4–C_5) part, whereas **7d** (or **10c**) is not. That is, one can expect that the transition state is stabilized considerably due to the conjugation and the energy barrier is lowered. Therefore, the 2,4 transposition is favorable in **1c** (path 3) and the 3,5 transposition in **1d** (path 4).

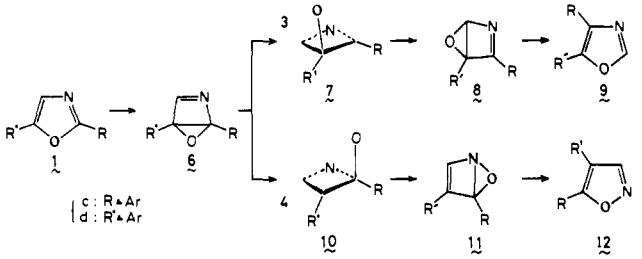

Concluding Remarks

In this paper the reaction mechanisms of photoisomerization of oxazoles are discussed on the basis of the results of ab initio MO-CI calculations. Four possible reaction paths are proposed and summarized pictorially in Figure 11. One of factors that controls the reaction course is the position of an aromatic substituent. The stabilization due to the conjugation with an aromatic substituent lowers the energy barrier to make the reaction favorable.

Though the basis set and the configuration selection employed in this work might not be sufficient to predict the reaction course quantitatively, the present calculation could describe the important features of the reaction mechanisms.

Acknowledgment. We thank the Computer Center of the Institute for Molecular Science for the use of the HITAC M-200H computer and the Library Program IMSPAC written by Prof. K. Morokuma and co-workers (IMS). We also express our gratitude to the Data Processing Center of Kyoto University for the use of the FACOM M-200 computer. This study was partly supported by a Scientific Research Grant (56540282) from the Ministry of Education of Japan.

Registry No. **1a**, 288-42-6; **2a**, 68289-74-7; **4a**, 84648-81-7; **6a**, 84648-82-8; **7a**, 84648-83-9; **10a**, 84648-84-0; **11a**, 84648-85-1.

Cyclic D_{6h} Hexaazabenzene—A Relative Minimum on the N_6 Potential Energy Hypersurface?

Paul Saxe and Henry F. Schaefer III*

Contribution from the Department of Chemistry and Lawrence Berkeley Laboratory, University of California, Berkeley, California 94720. *Received July 12, 1982*

Abstract: Vogler has recently reported laboratory evidence for the formation of hexaazabenzene from photochemical elimination in *cis*-diazidobis(triphenylphosphorane)platinum(II). Previous theoretical studies have suggested that the D_{6h} benzene-like structure is not a minimum on the N_6 potential energy hypersurface. Here the N_6 problem has been addressed at the self-consistent-field (SCF) level of theory using double-ζ (DZ) and double-ζ plus polarization (DZ+P) basis sets. The smaller basis set yields the prediction that the D_{6h} structure is a transition state connecting two equivalent bond alternant N_6 equilibrium geometries. A second transition state for dissociation to three nitrogen molecules (which are energetically much lower than N_6) was also located. Contrary to previous theoretical work, hexaazabenzene is found to be a minimum at the highest completely consistent level of theory. The equilibrium geometry occurs for r_e(N–N) = 1.288 Å, a bond distance suggesting that N_6 is a classic aromatic molecule. The transition state to $3N_2$ lies 10.3 kcal higher and has the planar, bond alternant structure, r_1 (N–N) = 1.178 Å, r_2(N–N) = 1.551 Å. Harmonic vibrational frequencies for hexaazabenzene are predicted with both theoretical methods and demonstrate that the energy surface is very flat with respect to bond alternating B_{2u} displacements. The inclusion of correlation effects lowers the barrier to N_6 dissociation when geometrical structures obtained at the SCF level of theory are assumed.

Introduction

The N_6 molecule hexazine or hexaazabenzene is the final member of the series of aromatic and potentially aromatic molecules **1**–**7**. In this series of 13 unsubstituted compounds,

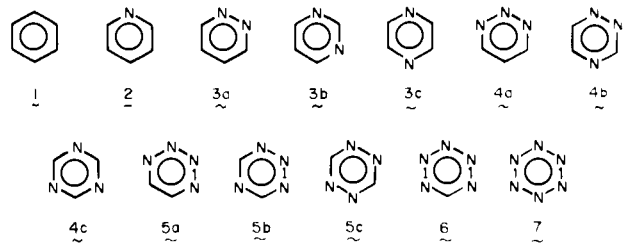

7 are well known and at least reasonably stable:[1,2] benzene (**1**), pyridine (**2**), pyridazine (**3a**), pyrimidine (**3b**), pyrazine (**3c**), *s*-triazine (**4c**), and *s*-tetrazine (**5c**). The eighth and last known compound of the series, 1,2,4-triazine (**4b**), was synthesized in 1966,[3] and an improved synthesis was reported in 1974,[4] but **4b** is apparently not well known, since a recent review[1] states that "the parent of this class has never been prepared".

(1) A. E. A. Porter, "Comprehensive Organic Chemistry", Vol. 4, D. Barton and W. D. Ollis, Eds., Pergamon Press, Oxford, 1979, pp 145–154.
(2) H. Neunhoeffer and P. F. Wiley, "Chemistry of 1,2,3-Triazines, 1,2,4-Triazines, Tetrazines, and Pentazines", Wiley, New York, 1978.
(3) W. W. Paudler and J. M. Barton, *J. Org. Chem.*, **31**, 1720 (1966).
(4) D. Krass and W. W. Paudler, *Synthesis*, **6**, 351 (1974).

0002-7863/83/1505-1760$01.50/0